SPECIAL FEATURE

Deep learning of spontaneous arousal fluctuations detects early cholinergic defects across neurodevelopmental mouse models and patients

Pietro Artoni[a], Arianna Piffer[a], Viviana Vinci[a], Jocelyn LeBlanc[a,b], Charles A. Nelson[b,c], Takao K. Hensch[a,c,d], and Michela Fagiolini[a,c,1]

[a]F. M. Kirby Neurobiology Center, Department of Neurology, Boston Children's Hospital, Boston, MA 02115; [b]Division of Developmental Medicine, Boston Children's Hospital, Boston, MA 02115; [c]International Research Center for Neurointelligence, University of Tokyo Institutes for Advanced Study, Tokyo 113-0033, Japan; and [d]Department of Molecular and Cellular Biology, Harvard University, Cambridge, MA 02138

Edited by Marla B. Sokolowski, University of Toronto, Toronto, ON, Canada, and accepted by Editorial Board Member Gene E. Robinson June 21, 2019 (received for review January 4, 2019)

Neurodevelopmental spectrum disorders like autism (ASD) are diagnosed, on average, beyond age 4 y, after multiple critical periods of brain development close and behavioral intervention becomes less effective. This raises the urgent need for quantitative, noninvasive, and translational biomarkers for their early detection and tracking. We found that both idiopathic (BTBR) and genetic (CDKL5- and MeCP2-deficient) mouse models of ASD display an early, impaired cholinergic neuromodulation as reflected in altered spontaneous pupil fluctuations. Abnormalities were already present before the onset of symptoms and were rescued by the selective expression of MeCP2 in cholinergic circuits. Hence, we trained a neural network (ConvNetACh) to recognize, with 97% accuracy, patterns of these arousal fluctuations in mice with enhanced cholinergic sensitivity (LYNX1-deficient). ConvNetACh then successfully detected impairments in all ASD mouse models tested except in MeCP2-rescued mice. By retraining only the last layers of ConvNetACh with heart rate variation data (a similar proxy of arousal) directly from Rett syndrome patients, we generated ConvNetPatients, a neural network capable of distinguishing them from typically developing subjects. Even with small cohorts of rare patients, our approach exhibited significant accuracy before (80% in the first and second year of life) and into regression (88% in stage III patients). Thus, transfer learning across species and modalities establishes spontaneous arousal fluctuations combined with deep learning as a robust noninvasive, quantitative, and sensitive translational biomarker for the rapid and early detection of neurodevelopmental disorders before major symptom onset.

transfer learning | LYNX1 | CDKL5 disorder | Rett syndrome | MECP2

Neurodevelopmental disorders on the autism spectrum (ASD) are heterogeneous. They are characterized by common deficits in social and communicative abilities as well as the presence of repetitive and restricted behavior (1–3). Both genetic and environmental factors contribute (1) to disorder onset in the first years of life, yet a diagnosis of ASD is typically not formulated before the age of 4 y. At present, the most effective clinical interventions are applied behavioral analysis and speech and occupational therapies, but treatment timing is critical before the highly plastic windows of brain development rapidly close. While early detection is clearly beneficial, the necessary noninvasive, quantitative, and sensitive biomarkers reflecting key circuits that are altered broadly across disorders are lacking.

The cholinergic circuit widely innervates brain regions to control (along with noradrenaline) many functions, like pupillary and cardiac oscillations (4–8). These are peripheral proxies for arousal fluctuations in the autonomic nervous system, the primary mechanism subserving the fight-or-flight response. Arousal oscillations mirror performance changes in cortical processing (5, 9), hippocampal activity in mice (5), and the encoding of memories in humans (10). Measuring arousal oscillations may then offer an opportunity to detect alterations that mouse models and ASD patients might share.

Indeed, individuals on the autistic spectrum exhibit dysregulated behavioral states in adulthood profoundly impacting their life (11–14), although we do not know when such altered states first arise. Among several neuromodulatory systems, the cholinergic system seems to be strongly and consistently perturbed in ASD (15–22). Namely, cholinergic neurons in the basal forebrain of ASD patients are altered in size, number, and structure (19). Concentrations of choline, a precursor of acetylcholine (ACh), are also decreased in patients with ASD and related disorders (20–24).

Spontaneous oscillations in pupil size are one-dimensional time series that represent a clear proxy of arousal (4, 5, 9), which can be measured across species since no specific task is involved. Furthermore, arousal fluctuations may contain additional unknown information that cannot be observed by conventional time domain or frequency domain analysis. Deep learning, with its natural application to biology (25) and medicine (26), is the ideal method for robustly extracting complex features of arousal dynamics characteristic of brain dysfunction.

Significance

Neurodevelopmental spectrum disorders such as autism (ASD) are typically diagnosed at an age beyond the heightened plasticity of the infant brain, when behavioral intervention would be most effective. Here, we show that mouse models of idiopathic or monogenic ASD share common alterations in arousal modulation that can be detected by machine learning early in life. In this transfer study across species and measures, we show that a neural network trained on mice can be refined by transfer learning to be useful for ASD patients, even when different proxies of arousal fluctuations are used (e.g., pupillometry or heart rate variation). This now offers a quantitative, noninvasive, and highly translational biomarker for the early detection of developmental disorders.

Author contributions: P.A., C.A.N., T.K.H., and M.F. designed research; P.A., A.P., V.V., and J.L. performed research; P.A. and M.F. analyzed data; and P.A., C.A.N., T.K.H., and M.F. wrote the paper.

The authors declare no conflict of interest.

This article is a PNAS Direct Submission. M.B.S. is a guest editor invited by the Editorial Board.

[1]To whom correspondence may be addressed. Email: michela.fagiolini@childrens.harvard.edu.

This article contains supporting information online at www.pnas.org/lookup/suppl/doi:10.1073/pnas.1820847116/-/DCSupplemental.

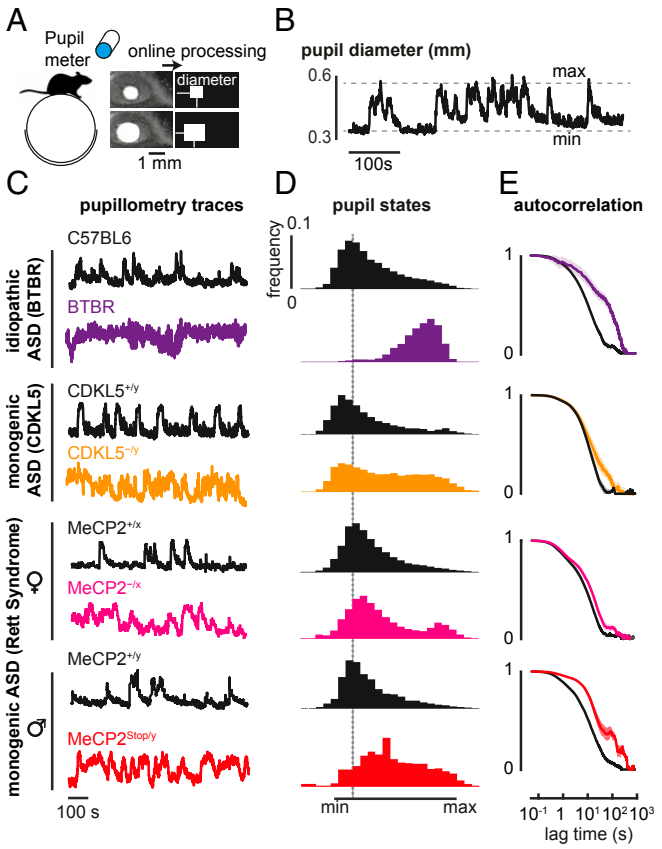

Fig. 1. Idiopathic and monogenic mouse models of ASD show prolonged and frequent high-arousal states. (*A*) Schematic of the experiment. Pupil traces are recorded from an awake mouse moving freely on a spherical treadmill, during a 30-min session. (*B*) Pupil diameter trace from a WT mouse. (*C*) Example of normalized pupil diameter traces from adult idiopathic (BTBR) and monogenic mouse lines (CDKL5 disorder and Rett syndrome), and their respective controls (C57BL6 and WT littermates). (*D*) Mean histogram of normalized pupil states across different mice. (*E*) Autocorrelation of the normalized pupil diameter traces, between ASD model and control mice. Shaded lines indicate SEM. Number of mice: P90 C57BL6 = 8, BTBR = 5, CDKL5$^{+/y}$ = 5, CDKL5$^{-/y}$ = 5; P100 MeCP2$^{+/x}$ = 6, MeCP2$^{-/x}$ = 8; >P60 MeCP2$^{+/y}$ = 9, P90 MeCP2$^{Stop/y}$ = 4.

Here, we evaluated spontaneous arousal fluctuations in both idiopathic and syndromic mouse models of ASD. We recorded the adult inbred BTBR$^{T+ltpr3tf/J}$ (BTBR) mouse strain (27) and 2 monogenic models of ASD-like Rett syndrome (RTT) and CDKL5 disorder (CDD), respectively, the MeCP2- (23, 28, 29) and CDKL5-deficient animals (30, 31). As neurotypical controls, we used either the C57BL6/J strain for BTBR animals or wild-type (WT) littermates of CDKL5- and MeCP2-deficient lines. All experiments and data analyses were conducted blind to genotype.

The BTBR strain has been characterized as a preclinical model of core behavioral deficits seen in autism, including repetitive behaviors and impaired sociability and vocal communication (27). *MECP2* gene mutations or changes in gene activity have been reported in some ASD cases, moderate to severe X-linked intellectual disability, severe neonatal encephalopathy, and, more commonly, Rett syndrome. Mice lacking MeCP2 faithfully recapitulate the human condition as characterized by an initial apparently normal development followed by regression, loss of acquired skills, and onset of autistic features and epilepsy (24). *CDKL5* mutations have been found in CDD patients and in subjects with neurodevelopmental disorders including ASD, atypical Rett syndrome, and early infantile epileptic encephalopathy. Mice lacking CDKL5 display a broad spectrum of behavioral abnormalities, including impaired learning and memory and autistic-like phenotypes (31–33).

After implantation of a head bar (*SI Appendix*), mice were habituated to moving freely on a spherical treadmill (Fig. 1*A*). Recordings of pupil diameter were acquired by an infrared camera, analyzed online during a 30-min session (Fig. 1*A*), and repeated multiple times over several days during the active phase of the light/dark cycle. Pupil traces (Fig. 1*B*) were normalized between the minimum and maximum value during each session as shown in Fig. 1*C*, to measure fluctuations between arousal states. In all ASD mouse models, we found a shifted distribution toward maximal pupil size with respect to WT controls (Fig. 1*D*), along with prolonged spontaneous fluctuations (Fig. 1*E*).

As it is unknown how early such an altered arousal phenotype can be detected from pupil fluctuations, we analyzed both male and female MeCP2-deficient mouse models of Rett syndrome, at postnatal ages before behavioral regression, when their RTT phenotypic score is still comparable to that of WT littermates (28, 29). Significant alterations in spontaneous pupillary fluctuations were found both in presymptomatic MeCP2$^{-/x}$ females (postnatal day, P45) and MeCP2$^{Stop/y}$ males (P30) (Fig. 2 *A*–*C*).

As it has recently been reported that young ASD patients exhibit altered pupillary response to visual stimuli (34, 35), we also evaluated this classical light-induced pupillary reflex (Fig. 2*D* and *SI Appendix*, Fig. S1 *A* and *B*). Strikingly, this failed to detect any abnormalities in presymptomatic mice (Fig. 2 *E* and *F*). Only at later stages of regression, when mice were already fully symptomatic, was a stronger pupil constriction and a slower poststimulus redilation observed (*SI Appendix*, Fig. S1*C*).

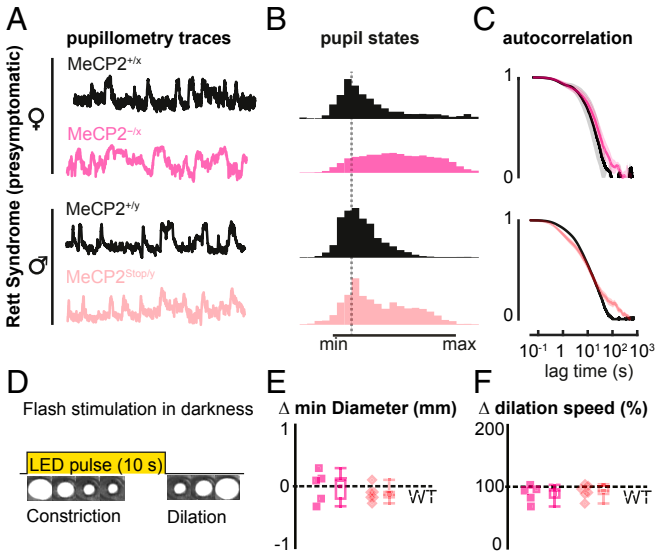

Fig. 2. Presymptomatic MeCP2 deficiency is reliably detected by spontaneous arousal oscillations but not by classical pupillary light reflex. (*A*) Normalized pupil fluctuations in MeCP2-deficient female (MeCP2$^{-/x}$, light magenta) and male (MeCP2$^{Stop/y}$, light red) mouse models of Rett syndrome at presymptomatic stage (postnatal day P45 and P30, respectively). (*B*) Mean histogram of normalized pupil states. (*C*) Autocorrelation traces of normalized pupil states. (*D*) Schematic of pupillary light reflex. Visible LED is briefly pulsed onto the eye of an awake mouse in total darkness. (*E*) Minimum pupil diameter and (*F*) redilation speed for MeCP2-deficient mice with respect to WT littermates (dashed line, WT baseline for each genotype). Each data point indicates average value measured from each mouse. Whiskers indicate the minimum and maximum values of the data, while boxes indicate the SD. Number of mice (each): P45 MeCP2$^{+/x}$ and MeCP2$^{-/x}$ = 5; P30 MeCP2$^{+/y}$ and MeCP2$^{Stop/y}$ = 7.

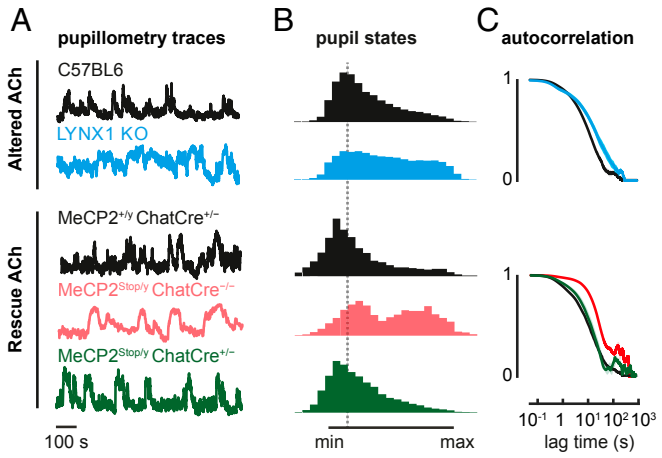

Fig. 3. Altered cholinergic tone prolongs high-arousal states in LYNX1 KO and MeCP2$^{Stop/y}$ mice. (*A*) Normalized pupillometry traces of P90 LYNX1 KO mice (cyan), age-matched C57BL6 controls (black), and adult (P60) MeCP2$^{Stop/y}$::ChatCre$^{+/–}$ mice (green), in which MeCP2 expression is rescued only in cholinergic cells. Two MeCP2 control littermates are shown: MeCP2$^{+/y}$::ChatCre$^{+/–}$ positive (black) and MeCP2$^{Stop/y}$::ChatCre$^{–/–}$ null (light red). (*B*) Mean histogram of normalized pupil states. (*C*) Autocorrelation traces of normalized pupil states. Number of mice: P90 C57BL6 = 8, LYNX1 KO = 6; P60 MeCP2$^{+/y}$::ChatCre$^{+/–}$ = 5, MeCP2$^{Stop/y}$::ChatCre$^{–/–}$ = 3, MeCP2$^{Stop/y}$::ChatCre$^{+/–}$ = 4.

Notably, MeCP2-deficient mice also showed longer locomotory bouts in their home cage throughout disorder progression despite their reduced speed and motor deterioration during later symptomatic stages (*SI Appendix*, Fig. S2). Together, these results support the idea of precociously altered arousal states in MeCP2-deficient mice, which can be reliably detected by spontaneous arousal fluctuations but not by classical pupillary reflex.

To test whether these alterations in arousal dynamics might reflect cholinergic circuit alterations, we ran 2 sets of experiments. First, we measured spontaneous arousal fluctuations in knockout (KO) mice lacking LYNX1, a protein that dampens nicotinic ACh receptor function in adulthood (36). Similar to the ASD model mice, adult LYNX1 KO mice exhibited a shifted distribution toward maximal pupil size with respect to C57BL6/J (Fig. 3). Spontaneous fluctuations also differed specifically in the slow temporal regime (oscillations > 1 s) across all mouse models (Figs. 1*C*, 2*C*, and 3*C*), in agreement with enhanced cholinergic signaling described in LYNX1 KO mice (4, 36) (Fig. 3*C*). This is consistent with cholinergic circuits mediating pupillary fluctuations (37–40) and altered cholinergic drive in both BTBR and RTT mouse models (27, 39–42).

Second, we aimed to directly rescue a cholinergic mechanism underlying the shared arousal phenotype. We took advantage of the MeCP2$^{Stop/y}$ line and bred them with a CHAT-Cre line (MeCP2$^{Stop/y}$::ChatCre$^{+/–}$), allowing selective expression of MECP2 only in cholinergic circuits. This targeted rescue was sufficient to prevent the arousal fluctuation phenotype (Fig. 3), while these mice continued to develop hindlimb clasping and motor deficits (39, 42). In addition, impaired pupillary reflex, further indicative of cholinergic impairment, was observed in LYNX1 KO mice and rescued in the MeCP2$^{Stop/y}$::ChatCre$^{+/–}$ line (*SI Appendix*, Fig. S1*C*). Overall, these results support the idea that altered cholinergic signaling underlies the abnormal arousal fluctuations seen in ASD and related disorders.

To distinguish between control and altered spontaneous pupil size fluctuations more objectively, we trained convolutional neural networks (ConvNets) on the data collected from LYNX1 KO mice to quantify the magnitude of cholinergic alterations in ASD mouse models. This ConvNetACh was composed of 4 convolutional layers and 2 fully connected layers, then fed with 32-s-long pupil traces, randomized in order, and shuffled in type for training (WT, black; LYNX1 KO, cyan, Fig. 4*A*; details in *SI Appendix*). After training on the categorization task of distinguishing WT from LYNX1 KO mice using 75% of the pupillometry data, we found that some nodes in the first ConvNetACh layer spontaneously developed selective sensitivity to multiple pupil parameters, while deeper layers developed sensitivity to single-event

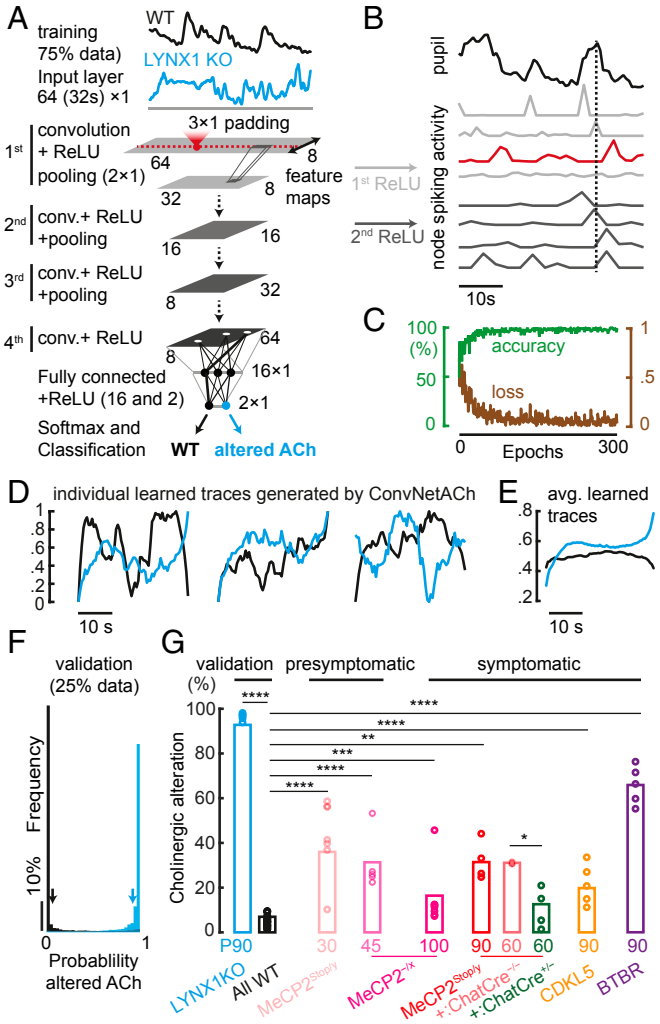

Fig. 4. Deep learning detects arousal alterations in mouse models of ASD. (*A*) Schematic of the model. A convolutional neural network for measuring cholinergic alterations (ConvNetACh), made of 4 convolutional layers and 2 fully connected layers, is fed with 32-s-long pupil traces, randomized in order, and shuffled in type for training (WT, black; LYNX1 KO, cyan). (*B*) The ConvNet develops receptive fields necessary for the discrimination of control from altered pupil fluctuations. (*C*) Measure of accuracy and loss during the training process (300 epochs), using 30 WT (~30,000 traces) and 6 LYNX1 KO mice (~8,000 traces). (*D*) Representation of individual learned WT and LYNX1 KO traces generated by the ConvNetACh using the DeepDream algorithm. (*E*) Representation of the average trace for one WT and LYNX1 KO mouse. (*F*) Validation of the model. Histogram of the responses of the network when it is fed with new data. Horizontal scale is detection probability of "altered ACh" output (WT = 0; LYNX1 KO = 1). (*G*) Measurement of cholinergic alteration in mouse models of ASD (circles, individual mice). Kolmogorov–Smirnov nonparametric test: *P < 0.05; **P < 0.01; ***P < 0.001; ****P < 0.0001. Number of mice: P90 LYNX1 KO = 6, All WT = 45, P45 MeCP2$^{–/x}$ = 5, P100 MeCP2$^{–/x}$ = 8, P30 MeCP2$^{Stop/y}$ = 7, P90 MeCP2$^{Stop/y}$ = 4, P60 MeCP2$^{Stop/y}$::ChatCre$^{–/–}$ = 3, P60 MeCP2$^{Stop/y}$::ChatCre$^{+/–}$ = 4, P90 CDKL5$^{–/y}$ = 5, P90 BTBR = 5.

peaks. Specifically, the first layer (rectified linear unit, ReLU 1) became sensitive to multiple pupil dilations, peaks, and constrictions, while deeper layers (e.g., ReLU 2) detected single pupil dilation events (dilation, peak, constriction) and multiple pupil peaks (Fig. 4*B*).

A total of ∼60 h of pupillometry between all WT ($n = 30$, ∼45 h) and LYNX1 KO mice ($n = 6$, ∼15 h) were used for training, achieving an accuracy of 97% (Fig. 4*C*). Examples of individual network-generated WT and LYNX1 KO arousal patterns (*SI Appendix*), which strongly and selectively activate the response of either one or the other output of ConvNetACh, are shown in Fig. 4*D*. The mean of such network-generated arousal traces (Fig. 4*E*) represents the receptive field of the "neuron" and the average notion that the network developed to describe either the WT or "altered ACh" class.

Interestingly, the average pupil trace identified by ConvNetACh was higher in amplitude and more fluctuating in LYNX1 KO mice than in controls, and recapitulated the results found by conventional analysis of higher frequency of wider pupil state (Fig. 3*B*) and fluctuations in the <1-Hz regime (Fig. 3*C*). The network was also validated with independent WT and LYNX1 KO data (25% of total data). Fig. 4*F* shows the probability of detecting a pupil trace as belonging to a mouse with "altered ACh" (ideally, always 0 for WT and always 1 for LYNX1 KO mice).

ConvNetACh properly identified new traces as WT in 94% of cases, and new LYNX1 KO traces as "altered ACh" in 95% of cases. Once fully trained, the network was run on mice that were suspected to have cholinergic abnormalities. It measured the probability of an arousal fluctuation to be recognized as "Altered ACh." ConvNetACh found a significantly altered cholinergic tone in both syndromic and idiopathic ASD mouse models compared with WT. Data are summarized in Fig. 4*G*, both as the average of data from each genotype (bars) and as the prediction on single mice (circles).

Notably, ConvNetACh predicted the strongest ACh alteration in both presymptomatic male and female MeCP2-deficient mice, supporting the idea that this tool might be useful as an early biomarker. Among the adult cohorts, ConvNetACh gave the highest score to BTBR mice, followed by the $MeCP2^{stop/y}$ males, and then the CDKL5 KO mice. Notably, ConvNetACh specifically selected for the "altered cholinergic trait" of the disorder spectrum, as demonstrated by a lack of response to the case of $MeCP2^{Stop/y}$::$ChatCre^{+/-}$ mice, in which any cholinergic-mediated phenotype was rescued while preserving other RTT phenotypes (39, 42).

As pupillometry and heart rate cofluctuate both in mice and humans [*SI Appendix*, Fig. S3; heart rate variability (HRV)], they can be used as equivalent proxies of arousal (43). HRV, which consists of spontaneous modulation of the heart rate in wakefulness, is atypically steady in ASD (44). Here, HRV detected arousal alterations in female RTT patients. HRV data (one-dimensional time series) were collected from the heart rates in a population of 35 RTT patients at different regression stages (15 in stage II, 18 in stage III) and of 40 typically developing (TD) subjects, then normalized between the minimum and maximum values across a long recording session (∼1 h long).

Human HRV measures shared the analogous amplitude and temporal signature observed already in pupillometry data from adult LYNX1 KO and MeCP2-deficient mice over development (Fig. 5*A*), indicating that comparable robust cholinergic alterations were detectable across species by either proxy. RTT patients exhibited a shifted distribution toward maximal heartbeat with respect to TD subjects (Fig. 5*B*). Moreover, spontaneous HRV also differed in the temporal domain specifically in the slow regime (oscillations of >5 s), similar to LYNX1 KO and MeCP2-deficient pupillometry (Fig. 5*C*). Higher and prolonged arousal states were also detected independently from video

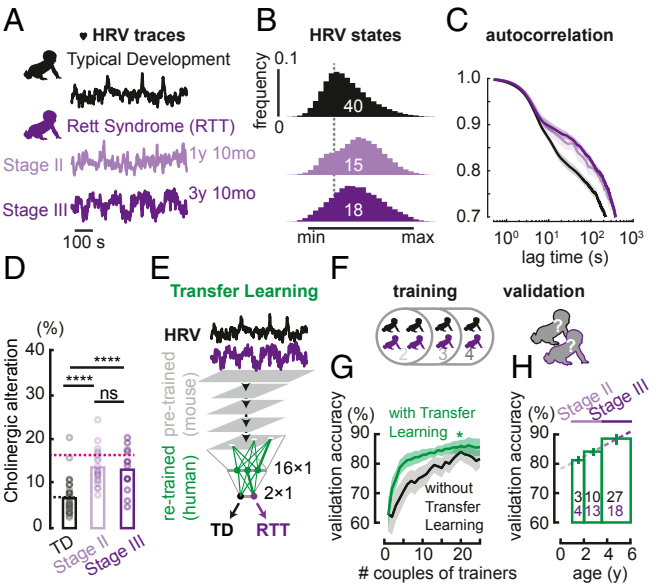

Fig. 5. Early detection of altered spontaneous arousal fluctuations in RTT patients using the neural network ConvNetPatients. (*A*) Example of normalized traces of spontaneous HRV in TD (black) and RTT (purple) subjects, across their regressive developmental trajectory. (*B*) Mean histogram of normalized HRV states in TD and RTT subjects. (*C*) Autocorrelation of normalized HRV traces, in TD and RTT subjects. Autocorrelation in the 0.5- to 3-s regime originates from a moving average in the algorithm that extracts HRV from the electrocardiogram. (*D*) Prediction of neuromodulatory alteration in TD and RTT subjects, using the ConvNetACh. Number of subjects: TD = 40, RTT Stage II = 15, RTT Stage III = 18; Mann–Whitney *U* test *P* values: TD-RTT Stage II ****$P = 4.5E-6$; TD-RTT Stage III ****$P = 8.9E-5$; RTT Stage II–RTT Stage III ns = 0.90. Black and pink dashed lines indicate average predictions for WT and P100 $MeCP2^{+/x}$ mice, respectively. (*E*) Transfer learning for training ConvNetPatients, consisting of a fast and selective retraining of only the very last layer of ConvNetACh. (*F*) Training strategy, consisting of training ConvNetPatients from HRV data of a randomly selected number of subjects (pairs of TD and RTT trainers), and validating accuracy on the remaining individuals (validators). (*G*) Validation accuracy (i.e., percent of TD and RTT patients properly identified by ConvNetPatients as a function of training size). Accuracy is shown in the case of transfer learning from ConvNetACh (green), and in the case of a clear and untrained network (black), repeating the training process for the same number of epochs. For each training size, an equal number of TD and RTT patients were randomly chosen as trainers for ConvNetPatients, which was then tested on the remaining subjects (validators). The random selection was iterated 10 times for each training size (among 40 TD and 35 RTT subjects), in consideration of the variability arising from the choice of trainers. (*H*) Validation accuracy by age (of validators), evaluated from a training size of 20 TD and RTT trainers each, randomly selected 50 times. Dashed line is fit to data across different age groups.

tracking data in all subjects (*SI Appendix*, Fig. S4 *A*–*C*) and appeared to be more pronounced at later RTT regression stages (*SI Appendix*, Fig. S4*D*).

Artificial neural networks carry great translational power because of their plastic capacity. Our neural network, reliably trained on mice, was also able to spot the same arousal alterations in RTT patients. By feeding ConvNetACh (previously trained on LYNX1 KO mouse data) with human HRV traces, we detected the altered arousal in RTT patients (Fig. 5*D*). Measurements of cholinergic alteration made by ConvNetACh for TD participants and RTT patients were close to those made, respectively, in WT and symptomatic $MeCP2^{-/x}$ female mice, the animal model closest to the RTT population of this study.

Finally, we investigated whether a ConvNet exploiting the information already learned from mice could identify subjects as TD or RTT, based only on their spontaneous arousal fluctuations

(Fig. 5*E*). For this purpose, a subset of human HRV traces was used to partially retrain the very last fully connected layers of the cholinergic-sensitive ConvNetACh (originally trained using LYNX1 KO and WT mice as described above). This transfer learning technique yielded ConvNetPatients, a neural network capable of classifying RTT patients from TD based on their spontaneous HRV.

To test the reliability of ConvNetPatients in a typical scenario of wide biomarker variability in patients, subjects were randomly divided into 2 groups: trainers, whose HRV data were used to train the neural network, and validators, who were then used for testing the accuracy of predictions made by ConvNetPatients (Fig. 5*F*). Since patient populations affected by rare neurodevelopmental disorders such as Rett syndrome are typically small, the accuracy of predictions by ConvNetPatients was also studied as a function of training size. As Fig. 5*G* shows, transfer learning from readily abundant mouse data (green) exhibited better performance than training a virgin neural network (black) over the same number of epochs.

To successfully learn from a very few patients while still correctly interpreting the data by inspecting specific units in a network, the network architecture must be kept simple. Thus, ConvNetACh and ConvNetPatients share the same simple architecture (Fig. 4*A*), compared with more complex ones typically used for image classification or speech recognition. This helps prevent overfitting and enables efficient transfer learning, potentially because the mouse data are less variable than in humans. Genetic mouse models carry exactly the same mutation, quite unlike patients who carry de novo mutations that generate a spectrum of phenotypes. This higher reproducibility of the mouse data is crucial to initiate the training process of the network toward a more solid and stable result, which can then be generalized by adding a second training with the human data. Conversely, a network trained exclusively on sparse patients would suffer from the intrinsic variability typical of human data, resulting in a less stable training process and, eventually, lower consistency in detecting arousal alterations.

In fact, the benefits of transfer learning dominate when the number of patients used for training the algorithm is small and the chance for highly discordant trainers is higher. Thus, a small training size (~10 pairs of TD subjects and RTT patients) was sufficient to achieve an accuracy of 82%, as opposed to barely 72% when transfer learning was not used. The former performance increases to 87% for a training size of 20 pairs (*SI Appendix*). In this case, with transfer learning (20 randomly selected TD subjects and RTT patients each), we measured an average accuracy of 80% even between 1- and 2-y-old individuals (Fig. 5*H*). By extrapolation, we can expect a detection accuracy of ~77% even in the first year of life, well before RTT is ever diagnosed. Moreover, the performance of ConvNetPatients increased with the number of patients, without ever reaching a clear plateau (Fig. 5*G*). Our proof-of-concept study encourages the expanded data collection from RTT or idiopathic ASD patients across clinical sites to further improve performance when using ConvNetPatients.

Overall, these results reveal that spontaneous arousal fluctuations are similarly altered in both syndromic and idiopathic ASD mouse models and in ASD-like RTT patients (Figs. 1 and 5). Arousal alterations are not dependent upon the proxy used to detect them (pupillometry or HRV) and are consistent across species, from mouse to human. Abnormalities can readily be detected in presymptomatic mice (Fig. 2), supporting spontaneous pupillometry as a practical and reliable early biomarker. Mechanistically, altered cholinergic drive is necessary and sufficient to reproduce the arousal fluctuations observed—mimicked by targeted deletion of the nicotinic receptor modulator LYNX1 and rescued by MeCP2 expression in the cholinergic source on an otherwise RTT background (Fig. 3). While altered cholinergic drive in BTBR and MeCP2-deficient mice has been documented (27, 39–42, 45–47), ours is an indication of a similar abnormality in CDKL5 mutants, suggesting further studies in preclinical and clinical setting.

Deep neural networks are flexible nonlinear classifiers that amplify subtle changes and detect even small aberrancies in arousal traces, learning from multiple individual fluctuations. Sophisticated enough to recognize patterns of pupil dilation and constriction, yet simple enough to be inspectable and allow learning from few samples without overfitting, the network must be trained on a dataset selected from models with known perturbations contributing to the phenotype. Here, we focused on a clear and specific discrimination clue of relevance to pupillometry, cholinergic enhancement in LYNX1 KO mice. We further showed that classical properties can still be extracted from these "black boxes" by inspecting the nodes in ConvNetACh. Average receptive fields for typical and "altered ACh" nodes satisfyingly converged to expected results, displaying higher pupil size and modulation in mice with cholinergic enhancement. Notably, the network was then able to capture the intrinsic variability of pupil fluctuations, as reflected in the heterogeneous pupil fluctuations generated by ConvNetACh for WT and LYNX1 KO mice (Fig. 4*D*).

ConvNetACh detected the very same "cholinergic signature" in presymptomatic MeCP2-deficient mice as well as in RTT patients. High accuracy and reproducibility were achieved through different levels of understanding of the "language" of spontaneous arousal fluctuations. In contrast, traditional pupillary reflex to light stimuli in presymptomatic MeCP2 mutant mice was unable to detect any difference compared with WT littermates. Moreover, the number of human trainers needed for ConvNetPatients to successfully discriminate TD from RTT patients was relatively small. This is particularly crucial for rare developmental disorders in which the training size can be limited. Given the straightforward, noninvasive nature of spontaneous arousal measures, cohorts of siblings at risk of developing ASD or carrying monogenic mutations like fragile X or tuberous sclerosis, in which only a subset of individuals go on to develop ASD, can now be pursued in large-scale studies across multiple sites.

We demonstrate transfer learning as an ideal choice for translational studies not just across species but also across the modality of measurement (e.g., pupillometry and heart rate). We found that spontaneous fluctuations of arousal are commonly altered in both idiopathic and genetic mouse models of ASD, both in the amplitude and temporal domain. These results illustrate the utility of this approach as a first-pass screening tool warning of impending neurodevelopmental abnormalities for timely intervention.

Materials and Methods

Mice. Mice were raised under standard laboratory conditions. Animal care and experimental procedures were performed in accordance with protocols approved by the Boston Children's Hospital Institutional Animal Care and Use Committee.

Human Participants. Data were recorded from 35 RTT girls and a control group of 40 TD girls with no history of prenatal or postnatal difficulties. All human procedures were reviewed and approved by the Boston Children's Hospital Office of Clinical Investigation and the institutional review board, and written informed consent was obtained from each participant or her guardian prior to testing.

Measurement of Spontaneous Pupil Fluctuations and Pupil Reflex. The pupil was imaged and tracked by an infrared camera. Pupil reflex was recorded in response to light-emitting diode (LED) stimulation.

Deep Learning Analysis. Traces were downsampled to 2 Hz, randomly segmented to 32 s length, and shuffled; 75% of the traces were used for training, while the remaining 25% were used for validation.

Statistics. The experimenter was blind to genotype during data acquisition, and no data points were rejected. The significance of the difference was established using the nonparametric 2-sample Kolmogorov–Smirnov test, and further confirmed by Wilcoxon signed rank sum test.

Transfer Learning. Transfer learning was performed using the Neural Network toolbox in MATLAB by retraining only the very last layer of the ConvNetACh, feeding the neural network with human HRV data.

Heart Rate Variation. The heart rate was used as a proxy of the arousal mostly for patients.

ACKNOWLEDGMENTS. We gratefully acknowledge support from the NVIDIA Corporation for the donation of a Titan Xp Graphics Processing Unit (GPU) used for this research. We also thank the Neurodevelopmental Behavioral Core of Boston Children's Hospital (BCH IDDRC 1U54HD090255) for technical support. T.K.H. is a Canadian Institute for Advanced Research (CIFAR) fellow. This work was supported by Human Frontier Science Program–Cross-Disciplinary Fellowship (HFSP-CDF) LT000975/2015C, Rettsyndrome.org, Italian Association of Rett Syndrome (AIRETT), NIH-National Institute of Neurological Disorders and Stroke Grant R01NS095959, World Premier International Research Center Initiative–International Research Center for Neurointelligence (WPI-IRCN) (Japan Society for the Promotion of Science), National Institute of Mental Health Silvio Conte Center Grant P50MH094271.

1. M.-C. Lai, M.-V. Lombardo, S. Baron-Cohen, Autism. *Lancet* **383**, 896–910 (2014).
2. R.-K. Lenroot, P.-K. Yeung, Heterogeneity within autism spectrum disorders: What have we learned from neuroimaging studies? *Front. Hum. Neurosci.* **7**, 733 (2013).
3. S.-S. Jeste, D.-H. Geschwind, Disentangling the heterogeneity of autism spectrum disorder through genetic findings. *Nat. Rev. Neurol.* **10**, 74–81 (2014).
4. J. Reimer *et al*., Pupil fluctuations track rapid changes in adrenergic and cholinergic activity in cortex. *Nat. Commun.* **7**, 13289 (2016).
5. M.-J. McGinley, S.-V. David, D.-A. McCormick, Cortical membrane potential signature of optimal states for sensory signal detection. *Neuron* **87**, 179–192 (2015).
6. A. Azarbarzin, M. Ostrowski, P. Hanly, M. Younes, Relationship between arousal intensity and heart rate response to arousal. *Sleep (Basel)* **37**, 645–653 (2014).
7. M. Ako *et al*., Correlation between electroencephalography and heart rate variability during sleep. *Psychiatry Clin. Neurosci.* **57**, 59–65 (2003).
8. G.-G. Berntson *et al*., Heart rate variability: Origins, methods, and interpretive caveats. *Psychophysiology* **34**, 623–648 (1997).
9. M. Vinck, R. Batista-Brito, U. Knoblich, J.-A. Cardin, Arousal and locomotion make distinct contributions to cortical activity patterns and visual encoding. *Neuron* **86**, 740–754 (2015).
10. M.-T. Kucewicz *et al*., Pupil size reflects successful encoding and recall of memory in humans. *Sci. Rep.* **8**, 4949 (2018).
11. E.-B. Prince *et al*., The relationship between autism symptoms and arousal level in toddlers with autism spectrum disorder, as measured by electrodermal activity. *Autism* **21**, 504–508 (2017).
12. A. Kylliäinen, J.-K. Hietanen, Skin conductance responses to another person's gaze in children with autism. *J. Autism Dev. Disord.* **36**, 517–525 (2006).
13. A. Kylliäinen *et al*., Affective-motivational brain responses to direct gaze in children with autism spectrum disorder. *J. Child Psychol. Psychiatry* **53**, 790–797 (2012).
14. N. Tinbergen, Ethology and stress diseases. *Science* **185**, 20–27 (1974).
15. K. Nakamura *et al*., Brain serotonin and dopamine transporter bindings in adults with high-functioning autism. *Arch. Gen. Psychiatry* **67**, 59–68 (2010).
16. E. B. London, Neuromodulation and a reconceptualization of autism spectrum disorders: Using the locus coeruleus functioning as an exemplar. *Front. Neurol.* **9**, 1120 (2018).
17. A.-P. Abdala, J.-M. Bissonnette, A. Newman-Tancredi, Pinpointing brainstem mechanisms responsible for autonomic dysfunction in Rett syndrome: Therapeutic perspectives for 5-HT_{1A} agonists. *Front. Physiol.* **5**, 205 (2014).
18. J.-C. Viemari *et al*., Mecp2 deficiency disrupts norepinephrine and respiratory systems in mice. *J. Neurosci.* **25**, 11521–11530 (2005).
19. T. L. Kemper, M. Bauman, Neuropathology of infantile autism. *J. Neuropathol. Exp. Neurol.* **57**, 645–652 (1998).
20. D. K. Sokol, D. W. Dunn, M. Edwards-Brown, J. Feinberg, Hydrogen proton magnetic resonance spectroscopy in autism: Preliminary evidence of elevated choline/creatine ratio. *J. Child Neurol.* **17**, 245–249 (2002).
21. S.-D. Friedman *et al*., Gray and white matter brain chemistry in young children with autism. *Arch. Gen. Psychiatry* **63**, 786–794 (2006).
22. G. L. Wenk, B. Hauss-Wegrzyniak, Altered cholinergic function in the basal forebrain of girls with Rett syndrome. *Neuropediatrics* **30**, 125–129 (1999).
23. R.-E. Amir *et al*., Rett syndrome is caused by mutations in X-linked MECP2, encoding methyl-CpG-binding protein 2. *Nat. Genet.* **23**, 185–188 (1999).
24. H. Leonard, S. Cobb, J. Downs, Clinical and biological progress over 50 years in Rett syndrome. *Nat. Rev. Neurol.* **13**, 37–51 (2017).
25. S. Webb, Deep learning for biology. *Nature* **554**, 555–557 (2018).
26. A.-L. Fogel, J.-C. Kvedar, Artificial intelligence powers digital medicine. *NPJ Digit. Med.* **1**, 5 (2018).
27. K. Z. Meyza, D. C. Blanchard, The BTBR mouse model of idiopathic autism–Current view on mechanisms. *Neurosci. Biobehav. Rev.* **76**, 99–110 (2017).
28. J. Guy, B. Hendrich, M. Holmes, J.-E. Martin, A. Bird, A mouse Mecp2-null mutation causes neurological symptoms that mimic Rett syndrome. *Nat. Genet.* **27**, 322–326 (2001).
29. J. Guy, J. Gan, J. Selfridge, S. Cobb, A. Bird, Reversal of neurological defects in a mouse model of Rett syndrome. *Science* **315**, 1143–1147 (2007).
30. I.-T. Wang *et al*., Loss of CDKL5 disrupts kinome profile and event-related potentials leading to autistic-like phenotypes in mice. *Proc. Natl. Acad. Sci. U.S.A.* **109**, 21516–21521 (2012).
31. E. Amendola *et al*., Mapping pathological phenotypes in a mouse model of CDKL5 disorder. *PLoS One* **9**, e91613 (2014).
32. C. Fuchs *et al*., Heterozygous CDKL5 knockout female mice are a valuable animal model for CDKL5 disorder. *Neural Plast.* **2018**, 9726950.
33. K. Okuda *et al*., Comprehensive behavioral analysis of the *Cdkl5* knockout mice revealed significant enhancement in anxiety- and fear-related behaviors and impairment in both acquisition and long-term retention of spatial reference memory. *PLoS One* **13**, e0196587 (2018).
34. E. Blaser, L. Eglington, A.-S. Carter, Z. Kaldy, Pupillometry reveals a mechanism for the Autism Spectrum Disorder (ASD) advantage in visual tasks. *Sci. Rep.* **4**, 4301 (2014).
35. P. Nyström *et al*., Enhanced pupillary light reflex in infancy is associated with autism diagnosis in toddlerhood. *Nat. Commun.* **9**, 1678 (2018).
36. J.-M. Miwa *et al*., The prototoxin lynx1 acts on nicotinic acetylcholine receptors to balance neuronal activity and survival in vivo. *Neuron* **51**, 587–600 (2006).
37. D.-E. Weese-Mayer *et al*., Autonomic nervous system dysregulation: Breathing and heart rate perturbation during wakefulness in young girls with Rett syndrome. *Pediatr. Res.* **60**, 443–449 (2006).
38. A. Kumar *et al*., Cardiovascular autonomic dysfunction in children and adolescents with Rett syndrome. *Pediatr. Neurol.* **70**, 61–66 (2017).
39. J.-A. Herrera, C.-S. Ward, X.-H. Wehrens, J.-L. Neul, Methyl-CpG binding-protein 2 function in cholinergic neurons mediates cardiac arrhythmogenesis. *Hum. Mol. Genet.* **25**, 4983–4995 (2016).
40. Y. Zhang *et al*., Loss of MeCP2 in cholinergic neurons causes part of RTT-like phenotypes via α7 receptor in hippocampus. *Cell Res.* **26**, 728–742 (2016).
41. S.-M. McTighe, S.-J. Neal, Q. Lin, Z.-A. Hughes, D.-G. Smith, The BTBR mouse model of autism spectrum disorders has learning and attentional impairments and alterations in acetylcholine and kynurenic acid in prefrontal cortex. *PLoS One* **8**, e62189 (2013).
42. H. Zhou *et al*., Selective preservation of cholinergic MeCP2 rescues specific Rett-syndrome-like phenotypes in MeCP2stop mice. *Behav. Brain Res.* **322**, 51–59 (2017).
43. Ş. Koç, S.-S. Baysal, K. Özbek, Does a change in iris diameter indicate heart rate variability? *Biomed. Res.* **29**, 1340–1344 (2018).
44. R. Thapa *et al*., Reduced heart rate variability in adults with autism spectrum disorder. *Autism Res.* **12**, 922–930 (2019).
45. G. Karvat, T. Kimchi, Acetylcholine elevation relieves cognitive rigidity and social deficiency in a mouse model of autism. *Neuropsychopharmacology* **39**, 831–840 (2014).
46. D.-A. Amodeo, J.-H. Jones, J.-A. Sweeney, M.-E. Ragozzino, Risperidone and the 5-HT2A receptor antagonist M100907 improve probabilistic reversal learning in BTBR T + tf/J mice. *Autism Res.* **7**, 555–567 (2014).
47. L. Wang *et al*., Modulation of social deficits and repetitive behaviors in a mouse model of autism: The role of the nicotinic cholinergic system. *Psychopharmacology (Berl.)* **232**, 4303–4316 (2015).